EPiC Series in Computing

Volume 114, 2026, Pages 115–124

Proceedings of the Workshop on Mathematical Modeling and Scientific Computing

2D Agent-Based Modeling of a Tumor Spheroid

Andrey Kovtanyuk[1,2], Aleksandra Gomziakova[1], and Valentin Andreev[1]

[1] Far Eastern Federal University, Vladivostok, Russia
kovtanyuk.ae@dvfu.ru, gomzyakova@yandex.ru, andreev.vy@dvfu.ru
[2] Technical University of Munich, Munich, Germany
kovtanyu@ma.tum.de

Abstract

An agent-based model describing the evolution of a tumor cell colony in a 2D domain is considered. The model incorporates the main cellular mechanisms responsible for tumor progression, namely proliferation, migration, and death. The spatial distribution of oxygen, which serves as a key nutrient for cell survival and growth, is modeled by a diffusion equation. The local oxygen concentration directly influences the transition probabilities of agents in the next phase of the cell cycle, as well as their migration and death.

To assess the macroscopic behavior of the system, the agent-based model is compared with a diffusion-type continuum model describing tumor development. This comparison makes it possible to analyze how stochastic cell-level interactions translate into large-scale tumor growth patterns. Numerical experiments demonstrate that reduced oxygen availability significantly alters the spatial structure and growth dynamics of the tumor colony.

1 Introduction

Almost all tumors undergo a stage of avascular growth, during which nutrients (for example, oxygen) are supplied from surrounding tissues. This process of avascular growth is more conveniently studied through experiments using *in vitro* tumor spheroids, which provide a reasonably accurate representation of the results and do not require extensive animal testing [7]. Tumor spheroids are characterized by a non-uniform distribution of oxygen and nutrients, leading to the formation of distinct cellular zones: a proliferating outer layer, an intermediate layer of quiescent cells, and a necrotic core [1]. Mathematical modeling of tumor evolution enables the development of therapeutic agents and the study of mechanisms underlying drug resistance and tumor progression.

Although biological tissues are inherently three-dimensional, 2D modeling remains highly relevant and practically significant in computational oncology, as it represents tumors as cross-sections and enables direct comparison with histological data [6]. Furthermore, 2D modeling significantly reduces computational costs, allowing rapid simulation of stochastic evolutionary scenarios for identifying fundamental spatiotemporal patterns prior to transitioning to complex three-dimensional systems.

This article focuses on the development and implementation of an agent-based modeling (ABM) algorithm. In recent years, ABM has emerged as a powerful paradigm in quantitative

V. Turova, A. Kovtanyuk, A. Maslovskaya and J. Zimmer (eds.), MMSC 2026 (EPiC Series in Computing, vol. 114), pp. 115–124

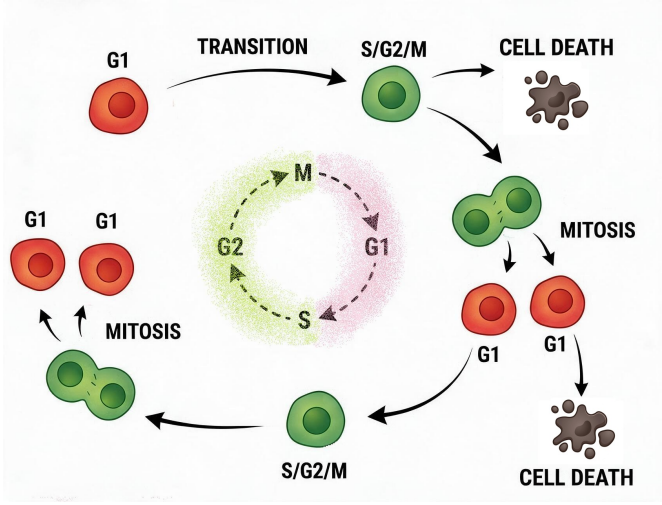


Figure 1: Cell cycle.

oncology, with frameworks ranging from lattice-based cellular automata to off-lattice center-based models. This study develops a hybrid algorithm combining ABM and oxygen diffusion [1]. At each time step, the oxygen distribution within the spheroid is calculated based on the diffusion equation. Then, using the resulting oxygen distribution in the spheroid, the probabilities of death, migration, and phase transition are calculated for each tumor. The results of ABM modeling are compared with the results of finite-element modeling based on a nonlinear diffusion model of tumor spheroid growth.

2 Tumor spheroid and cell cycle

Tumor spheroids are widely adopted to study avascular tumor growth and drug design [14]. The use of the Fluorescent Ubiquitination-based Cell Cycle Indicator (FUCCI) allows us to perform the real-time identification of the cell cycle for individual cells within a growing spheroid [9]. FUCCI allows us to distinguish between the following phases of the cell cycle, which, under fluorescent illumination, visualize the tumor cells in different colors. Thus, cells in phase G1 stain red, while cells in phase S/G2/M stain green. Cells in both phases can migrate and are also subject to death (phase D). When a cell dies, it ceases to exhibit any fluorescence upon irradiation; it appears black during visualization. Phase eS is sometimes also considered an intermediate phase between phases G1 and S/G2/M [12]. When irradiated, cells of the phase eS generate both red and green light; they appear yellow upon staining. In the subsequent modeling process, we will not distinguish a separate eS phase, instead assigning its cells to the combined S/G2/M phase.

The following cell cycle is typical for cells in a tumor spheroid (see Fig. 1 for illustration). Phase G1 cells can transition to phase S/G2/M. We assume that the transition rate is a given function of oxygen concentration c, denoted by K_u,

$$K_u(c) = \kappa_u c^s/(c_u^s + c^s), \tag{1}$$

where κ_u is the maximum rate of transition G1 $\to$ S/G2/M, s is a positive parameter and c_u is the critical concentration for the G1 $\to$ S/G2/M transition.

Cells in both phases G1 and S/G2/M can migrate and die. The migration and death rates are functions of oxygen concentration and are denoted by K_m and K_w, respectively,

$$K_m(c) = (\kappa_m - \gamma_m)\frac{c^p}{c_m^p + c^p} + \gamma_m, \tag{2}$$

$$K_w(c) = (\kappa_w - \gamma_w)\left(1 - \frac{c^q}{c_w^q + c^q}\right) + \gamma_w. \tag{3}$$

Here, κ_m is the maximum rate of migration, γ_m is the minimum rate of migration, κ_w is the maximum rate of death, γ_w is the minimum rate of death; p and q are positive parameters; c_m and c_w are the critical concentrations for migration and death, respectively.

3 Agent-based modeling

In the agent-based model, tumor cells are represented as discrete agents located at coordinates $\mathbf{x_n} = (x_n, y_n)$ for $n = 1, 2, ..., N(t)$, where $N(t)$ is the total number of tumor cells at time t. Also, we define by $N_u(t)$, $N_v(t)$, and $N_w(t)$ the number of tumor cells in G1, S/G2/M, and the death phase, respectively. We assume that at any given time moment, each cell is in one of three states: G1, S/G2/M, and D. A cell transitions from state G1 to state S/G2/M. Cells in state S/G2/M can be divided, producing two cells in state G1. Cells in states G1 and S/G2/M can die. When a cell dies, it is not removed from the simulation: the dead cell remains at its position as a static obstacle; it is taken into account when checking for available space to place other cells during the ABM process, but it does not migrate, divide, or consume oxygen.

Let $P_u(\Delta t)$, $P_v(\Delta t)$, $P_m(\Delta t)$, and $P_w(\Delta t)$ denote the probabilities of transition, mitosis, migration, and death events, respectively, over the time interval Δt. They are determined by known rates K_u, K_v, K_m, and K_w,

$$\begin{aligned} P_u &= 1 - \exp(-K_u\Delta t), \quad P_v = 1 - \exp(-K_v\Delta t), \\ P_m &= 1 - \exp(-K_m\Delta t), \quad P_w = 1 - \exp(-K_w\Delta t). \end{aligned} \tag{4}$$

Let the diameter of a tumor cell be d. We assume that during migration, the cell shifts in a random direction by a distance d, and during mitosis, the dividing cell remains at its position and returns to phase G1, while a daughter cell in phase G1 is placed at a distance d from it in a random direction.

The distribution of the normalized oxygen concentration c in the domain Ω with a boundary Γ is described by the following diffusion model:

$$-\Delta c + \alpha(u + v)c = 0, \quad c|_\Gamma = 1. \tag{5}$$

Here, α is the ratio of the oxygen consumption rate to the diffusion coefficient.

In the ABM of spheroid development, it is convenient to use an approximation corresponding to the case of central symmetry to determine the oxygen concentration. That is, the oxygen concentration $c(\mathbf{x}) \approx c_0(r)$, $r < R$, and

$$-c_0'' - c_0'/r + \alpha(u + v)c_0 = 0, \qquad c_0'(0) = 0, \qquad c_0(R) = 1, \tag{6}$$

where r is the distance from $\mathbf{x}$ to the center of the spheroid; $R = R(t)$ is the current radius of the spheroid defined as the 99th percentile of the distances of all living and dead cells from the center. The densities u and v are replaced by their averages over thin concentric rings. When

implementing the ABM algorithm, the solution of the boundary value problem (6) must be calculated at each time step, since u, v, and R depend on t.

As a result, we consider a hybrid ABM-diffusion model of the development of a tumor spheroid.

Algorithm 1. Hybrid ABM-diffusion algorithm

1: Set input data L, $R(0)$, $N_u(0)$, $N_v(0)$, $N_w(0)$, Δt, and number of iterations M.
2: Generate $N_u(0)$ cells of the phase G1, $N_v(0)$ cells of the phase S/G2/M, and $N_w(0)$ dead cells, uniformly distributed within the centered circle with radius R.
3: Initialize the counter $k = 0$.
4: From the diffusion model (6), find oxygen concentration c at time $t = k\Delta t$.
5: By formulas (1) – (4), calculate the probabilities P_u, P_v, P_m, and P_w.
6: By the probability P_u, play the transition event for each cell from phase G1 to phase S/G2/M.
7: By the probability P_w, play the death event for each cell of phases G1 and S/G2/M.
8: By the probability P_m, play the migration event for each cell of phases G1 and S/G2/M.
9: By the probability P_v, play the mitosis event for each cell from the S/G2/M phase, producing two G1 cells.
10: Check all cells for mutual overlaps. For cells with a center-to-center distance of less than 12 μm, shift them apart until the distance reaches 12 μm [8].
11: **if** $k = M$, **then** Stop.
12: **else** $k \leftarrow k + 1$; Go to 4.

Remark 1. *During migration and mitosis operations (steps 8 and 9), the algorithm first checks for available space. The applied criterion is that no more than five other cell centers lie within a radius of 18 μm around the position of the dividing cell (mitosis) or around the target position of the moving cell (migration). If this criterion is not met, the migration or mitosis event does not occur.*

Remark 2. *If mitosis is not possible for a cell in the S/G2/M phase due to the absence of free space, the cell transitions to the G1 phase [2].*

4 Diffusion model

We simulate the development of a 2D tumor spheroid of initial radius $R(0)$ centered in a square domain Ω with an edge L. Denote the boundary of Ω by Γ.

Let u, v, and w be the densities of tumor cells in the G1, S/G2/M, and death phases, respectively. The following system of PDEs describes their dynamics in the domain Ω [11]:

$$u_t - \nabla \cdot (D\,\nabla u) = 2K_v v - K_u u - K_w u, \tag{7}$$

$$v_t - \nabla \cdot (D\,\nabla v) = K_u u - K_v v - K_w v, \tag{8}$$

$$w_t = K_w u + K_w v, \tag{9}$$

where D is the diffusion coefficient. The transition rates K_u and K_w depend on the oxygen concentration c, that is, $K_u = K_u(c)$ and $K_w = K_w(c)$.

We supply the equations (7) – (9) the following initial and boundary conditions:

$$u(x,0) = u_0, \quad v(x,0) = v_0, \quad w(x,0) = w_0, \tag{10}$$

$$\partial_n u|_\Gamma = \partial_n v|_\Gamma = 0. \tag{11}$$

Unlike work [11], the diffusion coefficient D depends on the oxygen concentration, that is, $D = D(c)$ and it is found from the migration rate K_m and the migration shift d by the formula:

$$D = \frac{K_m d^2}{4}. \tag{12}$$

Note that (12) corresponds to an unobstructed random walk. In the ABM, a migration step is canceled when the target neighborhood is crowded (see Remark 1), so (12) is an upper estimate of the effective cell diffusivity inside the spheroid, where the actual mobility is lower.

The model (5), (7) – (11) is a non-linear diffusion model describing the development of a tumor spheroid. Its nonlinear character is determined by the nonlinear reaction term in (5) and the dependence of the rates K_u, K_m, K_w, and the diffusion coefficient D on the oxygen concentration c. It should be noted that the theoretical and numerical aspects of solving boundary-value, initial-boundary-value, and inverse problems for nonlinear diffusion models have currently been well studied (see, e.g., [3–5, 11]).

5 Numerical simulation

For numerical simulations, we consider a 2D spheroid with a radius of 250 μm centered in a square computational domain with an edge length of 1500 μm. At $t = 0$, we randomly generate 758 agents (tumor cells): 530 in G1 and 228 in S/G2/M. At each step of the ABM algorithm, the oxygen distribution within the computational domain is calculated by the diffusion model (5). Then, the probability of death or migration is determined for each agent (tumor cell). Additionally, for the G1 phase cells, the probability of transitioning to phase S/G2/M is found, while for cells in phase S/G2/M, the probability of mitosis resulting in the formation of two cells in the G1 phase is calculated. Based on the determined probabilities, the corresponding events (transition, death, migration, and mitosis) are played for each cell. The values of the problem parameters are listed in Table 1. The key parameters listed in the table are taken from [12], with the initial number of tumor cells adapted to the 2D geometry.

The ABM results were compared with the solution of the diffusion model (5) – (11) found using the finite element method with the applied software FreeFEM [10]. At each step of the ABM algorithm, the oxygen concentration is calculated by solving the boundary value problem (6) using second-order central finite differences on a uniform radial grid with 200 intervals, with the singularity at $r = 0$ eliminated by a symmetry condition; this yields a tridiagonal system of linear equations, which is solved using the Thomas algorithm.

Figures 2 (a) and (b) show the ABM results after 5 and 10 days, respectively. Phase G1 cells are represented by red dots, the phase S/G2/M cells by green dots, and dead cells by black dots.

The densities of live and dead cells after 5 and 10 days, obtained from the ABM results, are shown in Figs. 3(a) and (b), respectively. The figures demonstrate the migration of tumor cells and the formation of a necrotic core in the center of the spheroid. The development of the tumor spheroid is consistent with known experimental data [12, 13].

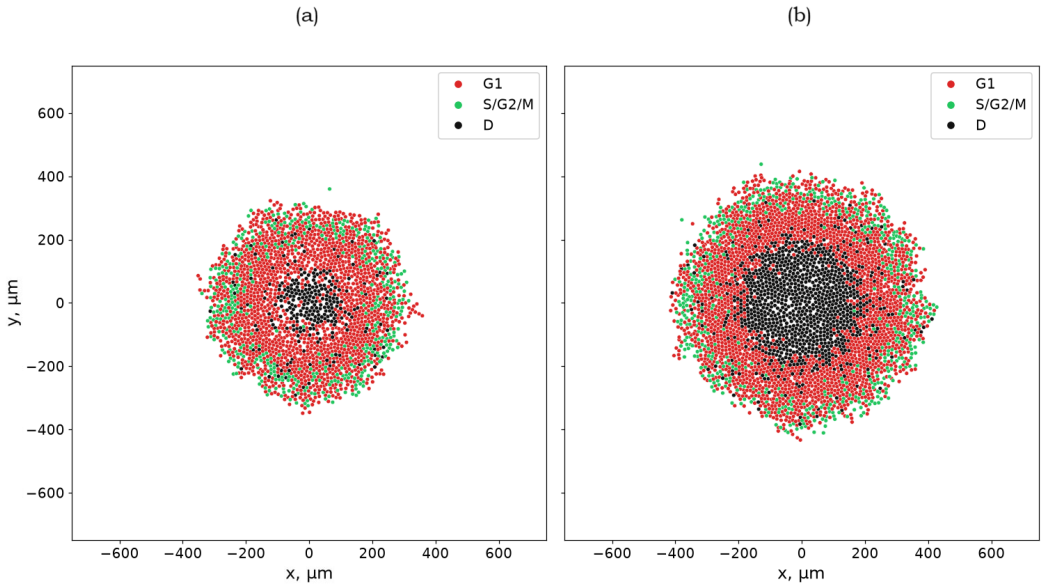


Figure 2: ABM results after: (a) 5 days and (b) 10 days.

Although both models (ABM and diffusion-based) show similar spheroid development, they also exhibit differences in solution behavior. Apart from the stochastic nature of the ABM as opposed to the deterministic continuum model, the two models differ structurally. In the ABM, mitosis and migration are subject to contact inhibition (see Remark 1): an event is canceled if more than five other cell centres lie within 18 μm, and an S/G2/M cell whose mitosis is blocked returns to the G1 phase (see Remark 2); moreover, dead cells remain in the spheroid as static obstacles and therefore also contribute to crowding.

The densities of live and dead cells obtained using the diffusion model demonstrate similar behavior (see Figs. 4(a) and (b)). The main differences are as follows. First, in the diffusion model, the necrotic core begins to appear as early as the first day. In contrast, in the ABM model, the necrotic core of the spheroid forms only on the 5th day, which is consistent with known experimental and computational data (see [12, 13]). From the 6th day, the density of necrotic cells in the spheroid core obtained using the ABM approaches the values predicted by the continuum model. A second difference lies in the different spheroid diameters demonstrated by the ABM and the diffusion model. The larger spheroid diameter predicted by the ABM can be attributed to the anisotropic character of cell migration. Due to the high cell density in the central region, including dead cells, and the lower density at the periphery, cells tend to migrate predominantly outward from the spheroid center. In contrast, in the diffusion model, dead cells are removed from the simulation and therefore do not hinder the migration of living cells toward the spheroid center. A more detailed comparison can be made by analyzing the cell densities in the central cross-section of the spheroid at the 5th and 10th days (see Figs. 5 and 6, respectively).

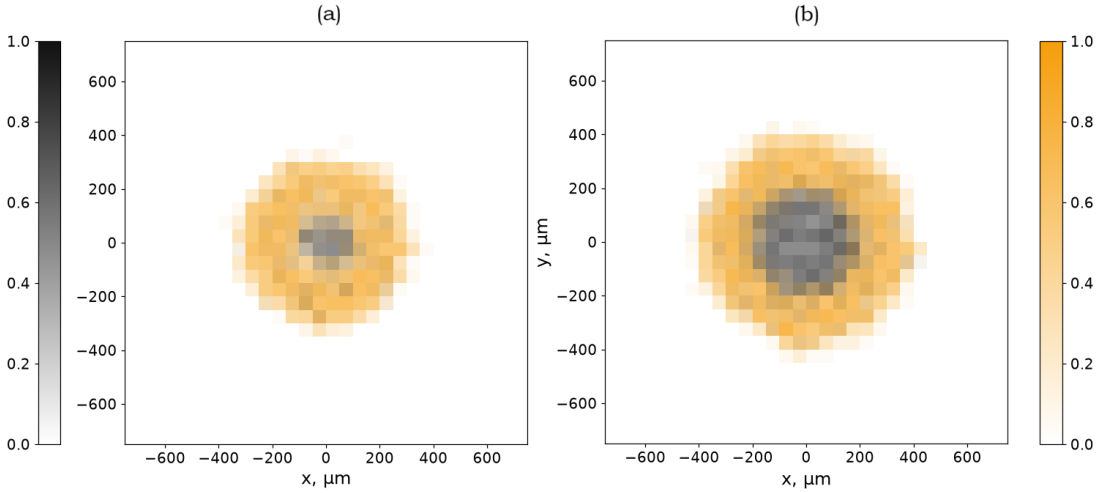


Figure 3: ABM results: density of living cells (shades of yellow) and density of dead cells (shades of gray) after 5 days (a) and 10 days (b).

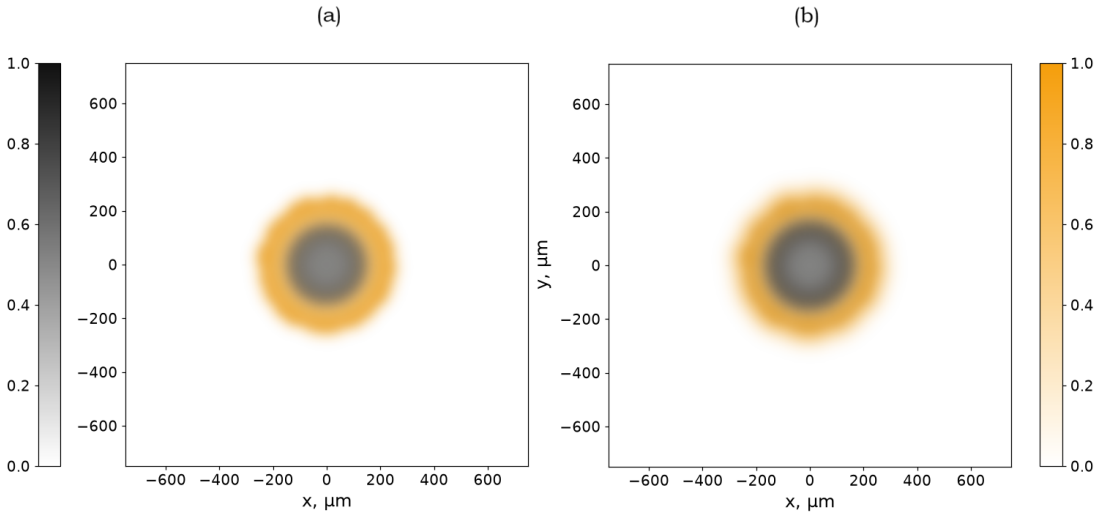


Figure 4: Diffusion modeling results: density of living cells (shades of yellow) and density of dead cells (shades of gray) after 5 days (a) and 10 days (b).

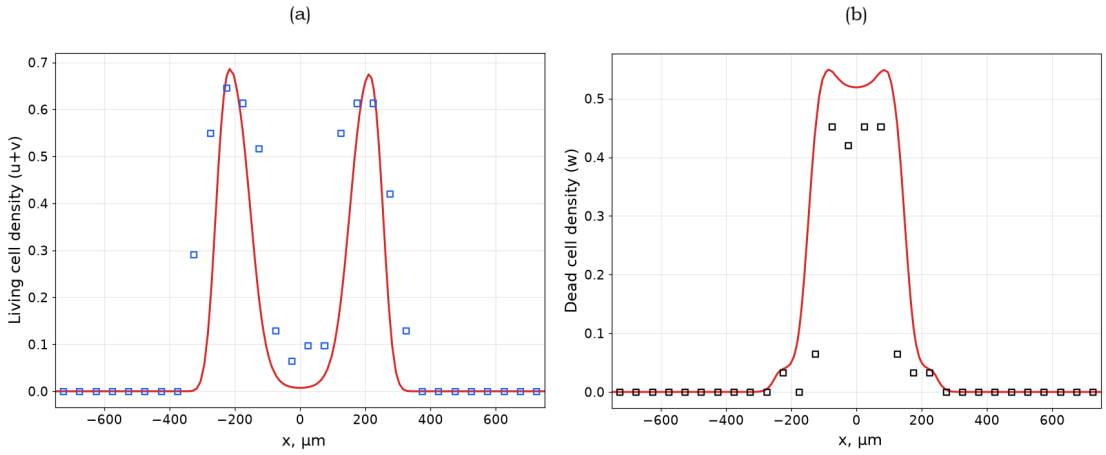


Figure 5: Comparison of ABM results (dot plot) and diffusion modeling (solid red line) in the central horizontal cross-section of the computational domain after 5 days: (a) density of living cell; (b) density of dead cells.

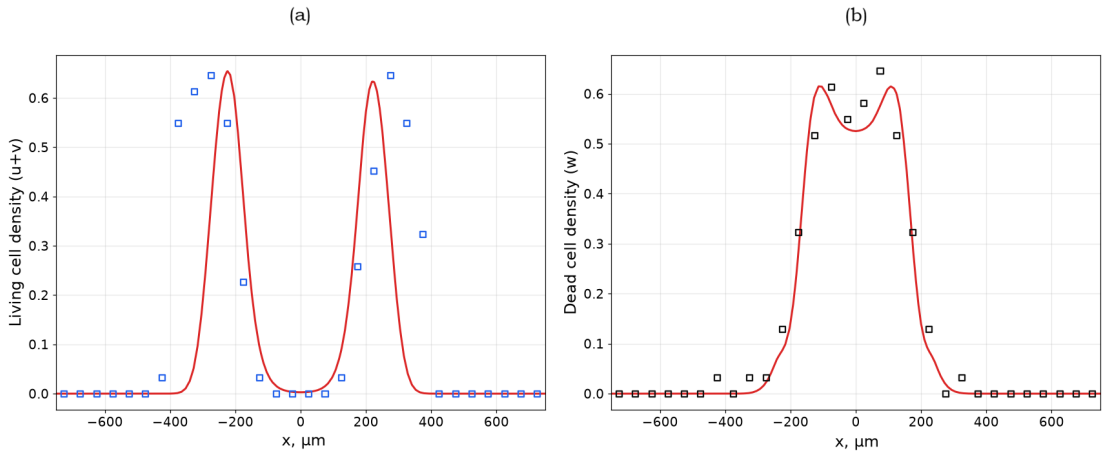


Figure 6: Comparison of ABM results (dot plot) and diffusion modeling (solid red line) in the central horizontal cross-section of the computational domain after 10 days: (a) density of living cell; (b) density of dead cells.

Table 1: Problem parameters.

Name	Description	Value	Units
L	Domain length	1500	μm
$R(0)$	Initial spheroid radius	250	μm
$N(0)$	Initial number of tumor cells (total)	758	–
$N_u(0)$	Initial number of G1 cells	530	–
$N_v(0)$	Initial number of S/G2/M cells	228	–
$N_w(0)$	Initial number of death cells	0	–
d	Cell diameter	12	μm
Δt	Time step	1	h
M	Number of iterations (10 days)	240	–
α	Ratio of the O_2 consumption rate to diffusion coefficient	2.0 e - 04	μm^{-2}
κ_u	Maximum rate of transition G1 $\rightarrow$ S/G2/M	0.047	h^{-1}
K_v	Mitosis rate	0.055	h^{-1}
κ_m	Maximum migration rate	0.12	h^{-1}
γ_m	Minimum migration rate	0.06	h^{-1}
κ_w	Maximum death rate	2.0	h^{-1}
γ_w	Minimum death rate	0.0005	h^{-1}
c_u	Critical cells concentration for the G1 $\rightarrow$ S/G2/M transition	0.4	–
c_m	Critical cells concentration for migration	0.5	–
c_w	Critical cells concentration for death	0.1	–
s	Hill function index for transition G1 $\rightarrow$ S/G2/M	5	–
p	Hill function index for migration	5	–
q	Hill function index for death	15	–

6 Conclusion

Agent-based models of tumor spheroid development allow for the explicit description of individual cell behavior, phenotypic diversity, and local interactions, making them particularly suitable for studying cellular heterogeneity, invasion, and the effects of therapy at the micro-level. Diffusion models based on partial differential equations effectively describe the macroscopic characteristics of a spheroid, such as averaged solution and nutrient concentrations, as well as changes in proliferation and necrosis zones. Although convenient for theoretical and numerical analysis, they do not allow for the direct incorporation of individual cell properties or significant spatial heterogeneity at the microscale. Thus, the choice between agent-based and diffusion-based approaches is determined by the research objectives: agent-based or hybrid models are preferable for tasks focusing on cellular mechanisms and heterogeneity, whereas continuum PDE models are suitable for describing global dynamics and substance profiles in large spheroids.

Acknowledgements

This work was supported by the Ministry of Science and Higher Education of the Russian Federation (Agreement No. 075-02-2026-1312).

References

[1] M. Amereh, R. Edwards, M. Akbari, and B. Nadler. In-silico modeling of tumor spheroid formation and growth. *Micromachines*, 12(7):749, 2021.

[2] D.R. Bergman, K.A. Norton, H.V. Jain, and T. Jackson. Connecting agent-based models with high-dimensional parameter spaces to multidimensional data using SMoRe ParS: A surrogate modeling approach. *Bull Math Biol.*, 86(1):11, 2023.

[3] R.V. Brizitskii and A.A. Donchak. Multiplicative control problem for a nonlinear reaction–diffusion model. *Comput. Math. Math. Phys.*, 64:56–72, 2024.

[4] R.V. Brizitskii, N.N. Maksimova, , and A.G. Maslovskaya. Theoretical analysis and numerical implementation of a stationary diffusion-drift model of polar dielectric charging. *Comput. Math. Math. Phys.*, 62:1680–1690, 2022.

[5] R.V. Brizitskii, N.N. Maksimova, , and A.G. Maslovskaya. Inverse problems for the diffusion-drift model of charging of an inhomogeneous polar dielectric. *Comput. Math. Math. Phys.*, 63:1685–1699, 2023.

[6] Y. Chen, H. Wang, J. Zhang, K. Chen, and Y. Li. Simulation of avascular tumor growth by agent-based game model involving phenotype-phenotype interactions. *Sci. Rep.*, 5:17992, 2016.

[7] N. Cogno, C. Axenie, R. Bauer, and V. Vavourakis. Agent-based modeling in cancer biomedicine: applications and tools for calibration and validation. *Cancer Biol. Ther.*, 25(1):2344600, 01 2024.

[8] B. Colyer, M. Bak, D. Basanta, and R. Noble. A seven-step guide to spatial, agent-based modelling of tumour evolution. *Evolutionary Applications*, 17:e13687, 2024.

[9] N.K. Haass, K.A. Beaumont, D.S. Hill, A. Anfosso, P. Mrass, Marcia A. Munoz, I. Kinjyo, and W. Weninger. Real-time cell cycle imaging during melanoma growth, invasion, and drug response. *Pigment Cell & Melanoma Research*, 27(5):764–776, 2014.

[10] F. Hecht. New development in FreeFEM++. *J. Num. Math.*, 20:251–265, 2012.

[11] W. Jin, L. Spoerri, N.K. Haass, and M.J. Simpson. Mathematical model of tumour spheroid experiments with real-time cell cycle imaging. *Bull. Math. Biol.*, 83:44, 2021.

[12] J.J. Klowss, A.P. Browning, R.J. Murphy, E.J. Carr, M.J. Plank, G. Gunasingh, N.K. Haass, and M.J. Simpson. A stochastic mathematical model of 4D tumour spheroids with real-time fluorescent cell cycle labelling. *Journal of The Royal Society Interface*, 19(189):20210903, 04 2022.

[13] X. Mao, S. McManaway, J.K. Jaiswal, P.B. Patel, W.R. Wilson, K.O. Hicks, and G. Bogle. An agent-based model for drug-radiation interactions in the tumour microenvironment: Hypoxia-activated prodrug SN30000 in multicellular tumour spheroids. *PLoS Comput Biol.*, 14(10):e1006469, 2018.

[14] A.S. Nunes, A.S. Barros, E.C. Costa, A.F. Moreira, and I.J. Correia. 3D tumor spheroids as in vitro models to mimic in vivo human solid tumors resistance to therapeutic drugs. *Biotechnology and Bioengineering*, 116(1):206–226, 2019.